Summary of Results and Conclusions Based on Analysis of Volume Imaging and High Spectral Resolution Lidar Data Acquired During FIRE Phase I: Part I

C. J. Grund and E. W. Eloranta
University of Wisconsin
Department of Meteorology
1225 West Dayton St.
Madison, WI 53706

I. Introduction

The collection of long term global statistics on cloud cover, a major goal of ISCCP, may (potentially) be most easily accomplished with satellite based observations; however, measurements derived from passive satellite retrieval methods must be calibrated and verified by insitu or ground based remote sensor observations. Verification is not straight forward, however, because the highly variable nature of cloud altitude, morphology, and optical characteristics complicates the scaling of point measurements to satellite footprint sized areas. This is particularly evident for cirrus clouds which may be organized on horizontal scales of 10's of meters to 100's of kilometers, may exhibit physical depths of 10's of meters to 8 km or more, and have optical depths ranging from less than .003 to greater than 3. Cirrus clouds can strongly influence earths' radiative balance, but, because they are often transmissive, cirrus clouds are difficult to detect and characterize from satellite measurements.

Because of its precise ranging capabilities, spatial resolution and sensitivity, lidar observations have played an important role in the detection, depiction, and characterization of cirrus clouds. This paper summarizes some of the characteristics of cirrus clouds observed by the University of Wisconsin High Spectral Resolution (HSRL) and Volume Imaging Lidars (VIL) during the phase I IFO and ETO periods. Because of the volume of material, we have split our presentation into two parts: an overview oral summary and a more detailed poster presentation. Since the VIL data are most easily summarized in a visual format unsuitable for reproduction here, we have primarily reported HSRL measurement contributions in this 2 part abstract. Both poster and oral presentations will include this additional material, as well as examples of new VIL and HSRL instrument capabilities.

II. U.W. Lidar Instrumentation

The University of Wisconsin lidar group operates two unique lidar systems: the High Spectral Resolution Lidar (HSRL) and the Volume Imaging Lidar (VIL).

The HSRL is optimized to produce calibrated measurements of optical depth, extinction corrected cloud morphology, and backscatter phase function[1] (determined by particle size, composition, and shape). The HSRL spectrally separates Doppler broadened molecular backscatter from unbroadened (primarily elastic) cloud particle and aerosol backscatter. Using the known distribution of molecular scattering cross section to provide a calibration reference at every range, extinction is unambiguously determined from the observed molecular backscatter intensity. HSRL measurements of cirrus cloud optical properties were first acquired during the FIRE cirrus IFO in 1986. Since then, the HSRL has routinely operated to collect statistics on cirrus optical properties and in support of VAS cloud height verification studies[2].

The VIL, is optimized for rapid scanning of large atmospheric volumes. A high repetition rate laser (30 Hz) coupled with fast scanning mirrors (25^{o} / sec) and a high speed data logging system (~.5 gigabyte/hr) writing to optical disk (2.6 gigabyte capacity) allow this system to produce 3-D reconstructions of cirrus cloud backscatter by assembling successive 2-D cross wind scans on a

graphics display terminal. Movie loops of successive wide angle scans taken along the mean wind direction reveal a mesoscale time history of cirrus evolution. From a single ground based location, the VIL can scan a 60 km wide segment of cirrus with 100 m resolution in 20 seconds. Cirrus data have been acquired with this system since the summer of 1987 in conjunction with specific field experiments.

III. Observed cirrus properties

a. Optically thin cirrus

Extensive fields of optically thin clouds are important for a number of reasons: background noise generated by thermal emissions from the cloud and ambient light scattered by the cloud can interfere with IR remote measurements, and, attenuation along shallow view angles, as in limb scanning, can become significant. If present globally, they may also have a significant impact on earths' radiative balance while going largely undetected by space-borne passive remote sensing techniques.

Plotted in fig.'s 1 and (2) are two of our best examples of this type of cloud. The data on these clouds were acquired during the FIRE IFO case study day[3] October 28, 1986. Solid lines represent backscatter cross section contours in 10^{-7} (10^{-8}) m^{-1} sr^{-1}. The dashed lines indicate optical mid-cloud altitude (half the cloud optical thickness is accumulated to either side of this line), and dotted lines are wind speeds in m/s. Because the HSRL cannot distinguish between backscatter from aerosols and that from cloud particles, we cannot be certain that these tenuous veils of enhanced backscatter are cirrus; however, since denser cirrus were observed at these altitudes both before and after this time period, these features at least appear to be associated with cirrus. Average layer optical thickness in the vertical was ~.01 (~.003). Wind-drift estimates suggest these layers extend for at least 266 km (180 km).

Isotachs plotted in fig. 1 from the special FIRE three-hourly radiosonde data show a general correlation between wind speed maxima and backscatter cross section contours (note the 26 m/s and 29 m/s patterns). Fig. 2 also suggests a correlation between wind sheer and backscatter cross section (note the region between 9.5 and 10.5 km at 1000 UTC). These apparent pattern correlations have been observed in several cases, though a consistent set of correlation characteristics has not been established. It is not certain if the sheer is part of the cirrus generation mechanism, or if cirrus formation and winds are both responding to the same environmental forcing.

b. *Mesoscale uncinus complex (MUC)*

Fig. 3 shows a contour map of a MUC[5] observed on October 28, 1986 from 0500 - 0900 UTC. GOES IR images of this phenomena, combined with radiosonde winds, suggest that the MUC is a south-eastward propagating cirrus generation region embedded in a less intense, generally eastward moving, wind-driven cloud band. The NW-SE oriented cloud band was part of a more extensive cloud shield covering northern Wisconsin. The GOES IR images show the MUC passed directly over Madison, with the radiance minima occurring ~0700 (interpreted as the densest cloud region, not necessarily the highest cloud top, as for opaque clouds).

A series of uncinus generating cells are evident between 9.5 and 11 km, particularly between 0530 and 0700. Each of these cells is about 150 m thick. Cloud translation with the 10 km wind (20 $ms^{-1} \pm 10$ ms^{-1}) would suggest the cells are ~4 - 12 km across; thus, they have a height to width aspect ratio in the range ~1:54 - 1:180. The maximum $\beta_{a\pi}/4\pi$ (normalized backscatter cross section) for this MUC was determined to be .024 km^{-1} sr^{-1} at 0722 near 8.7 km altitude, preceding the passage of a wind jet maximum of ~34 ms^{-1}. Both the Ft. McCoy and Platteville soundings at 0300 and 0900 (0600 was not acquired) indicate the regions above 7.4 km were consistently moist (>70% RH with respect to ice) and occasionally reached supersaturation as high as ~108 % with respect to ice. The radiosonde profiles also show an abrupt decrease in relative humidity below 7.4 km

suggesting the steep contour gradient at 0700 at 7.2 km altitude is related to rapid ice crystal evaporation in the dry environment beneath the complex. Profiles averaged from 0600-0750 indicate this system had a mean optical thickness of .58±0.05 which varied from 0.09±0.03 at 0750 to 1.1±0.3 at 0718. The bulk backscatter phase function averaged over the same time period was 0.042±0.015 sr^{-1}.

Isotachs, interpreted from the 0300 and 0900 Ft. McCoy radiosonde data, show an apparent relationship between wind speeds and the MUC backscatter cross section distribution. Note the close proximity in time and altitude between the wind speed maximum and the backscatter cross section maximum. Cloud bottom seems to occur where the time height cross section indicates relatively steady winds. The decrease in cloud top altitude seems to be related to the development of a wind minimum at 10.5 km. The jet and the wind minimum are of smaller scale than the FIRE IFO radiosonde network. They appear strongly only in the Ft. McCoy soundings, and are just discernible in the Platteville sounding data; thus, no attempt has been made to interpolate the radiosonde data to Madison observation times. Future observations of this type would benefit from a more dense temporal and spatial net of wind observations.

The MUC observations also demonstrate the limitations inherent in interpreting cirrus cloud morphology strictly from zenith time height cross section measurements. If the wind sheer is deduced from the apparent slope of the virga trails, the wind maximum would be expected near the upper cloud level at ~10 km. In fact, the wind contours indicate the maximum of ~35 m/s near 8.5 km, decreasing to ~18 m/s at 10 km. Clearly, the time height cross section of this complex does not represent a stationary phenomena translating with the ambient winds but that the clouds are undergoing significant evolution. Cloud genesis is probably related to circulations about the mesoscale jet, and the apparent shape of virga may be partially governed by the local distribution of moisture.

c. *Altocumulus vs. cirrus*

From 1200 - 1500 UTC on 10/28, a two level cirrus / alto-cumulus formation was observed. Fig. 4 highlights the dissimilarity in lidar backscatter between these cloud types. The lower layer cloud appears to be formed from a series of relatively dense alto-cumulus cells with a .5-1 km long ice crystal fallout tail (identification as ACu is inferred from an all-sky photograph taken at Wausau and the fact that similar cloud structure was observed at Ft. McCoy and Wausau lidar data around this time period[4]. Ice virga is inferred from the environmental temperature (-25^{o} to -30^{o} C) and from higher resolution images of lidar backscatter. Wind-drift estimates indicate the ACu were about 20 km across, yet they were ~200 m thick, producing a height to width ratio of only 1:100. As the ACu developed, fig. 5 shows an increase in both the total cloud optical thickness and the backscatter phase function while the optical mid-cloud altitude decreased from ~11 km to ~7.5 km. The average cloud backscatter phase function peaks with the passage of each ACu cell. Because similar cloud features were also observed to produce little depolarization at Wausau and Ft. McCoy, we can infer, with some confidence, that the backscatter phase function peaks suggest these clouds are composed of super-cooled spherical water droplets[4].

The ACu bands at ~7.6 km produce significantly greater backscatter than either the 9-12 km cirrus or the lower level virga between 6.4 and 7.1 km. The $\beta_{a\pi}/4\pi$ maximum reached at 1419 exceeded 0.15 km^{-1} sr^{-1}. One reason for this is that ACu are primarily composed of super-cooled liquid water droplets; because of optical surface wave phenomena, such droplets are more efficient at backscattering than non-spherical ice crystals. A second reason is that super-cooled water droplets are necessarily quite small, whereas, once glaciation begins, cloud particles accumulate mass rapidly because of the reduction of saturation vapor pressure with respect to ice; hence, ice particle fall speeds rapidly exceed vertical atmospheric motion, and particle mass distributes over an extended column, decreasing the local backscatter intensity. Since particle mass increases as the cube of the radius while the scattering cross section approximately follows the radius squared, the backscatter

cross section will also diminish as growth processes redistribute water mass from many small particles to fewer but larger ice crystals with substantial fall speeds.

The ACu dominate the optical thickness profile. Clearly, the occurrence of ACu can have significant impact on the radiative properties of the cloud independent of cloud top altitude and bottom altitudes.

d. *Cirrostratus*

Cirrus frequently form continuous layers with vertically developed cells of enhanced backscatter appearing near both cloud top and cloud bottom. Fig. 6 illustrates this type of formation observed on 10/28/86. The vertical elongation of backscatter cross section contours suggests an upward and/or downward redistribution of cloud particles. The top and bottom cellular morphology of this layer is most evident ~1610 where an apparent generating region near cloud top produces a virga trail which extends to, and perhaps seeds, a second region of strong backscatter near ~7.5 km. The lower regions (at 1610 and 1640) also appear to be precipitating as evidenced by the vertical elongation of the cloud bottom backscatter cross section contours. Note that the mid-cloud altitude follows regions of enhanced backscatter very closely and that there is no obvious relationship between the appearance of these regions and either cloud top or cloud bottom altitudes. Thus, the structures which dominate cloud optical properties are not necessarily indicated by either the cloud boundaries or the physical mid-cloud altitude.

With the exception of two periods, near 1540 and 1915, the cirrus optical thickness exceeded 0.1 forming an apparent cirrostratus layer (see fig. 7). The gap in cloud cover at ~1900 corresponds to the passage of a clear arc identified from satellite imagery[5]. Peaks in backscatter phase function (~.038 sr^{-1}) tend to coincide with the occurrence of the regions of enhanced backscatter cross section independent of total optical thickness, while the regions between the cells usually produce the minima in the backscatter phase function of ~.02 - .026 sr^{-1}. This suggests differences in the microphysical properties for the particles associated with the cells compared with those of the surrounding cloud. One explanation may be that the regions of enhanced backscatter are areas of cloud particle generation which may contain an abundance of small supercooled water droplets (temperature at 7.5 km: ~-30° C, at 9.5: ~-45° C). An abundance of particles approaching molecular diameters could also produce the observed backscatter phase function and depolarization ratio effects. Unfortunately, the issue cannot be settled by insitu probe data because current instruments are incapable of resolving such small particles. In regions between the cells, it may be that sufficient time has elapsed so that the number density of droplets has been substantially diminished by differential vapor pressure effects between ice and water. The modulation of the bulk backscatter phase function also suggests that some of the apparent structure observed in the backscatter cross section plots is generated by microphysical changes and is not simply related to the cloud extinction cross section. This effect should be considered when deducing cloud morphological and optical characteristics from simple plots of lidar backscatter .

The backscatter contours in fig. 6 indicate a large scale pattern of intensification with a period of about 45 minutes; however, an examination of the higher time resolution pictures of the raw laser returns reveals the clouds contain a finer scale (~5 minute) structure imbedded in the larger scale organization. Wind drift estimates would suggest that these features have a horizontal scale of about 9-11 km. Thus, the height to width aspect ratio of the elementary structures is ~1:5 while the larger scale field of enhanced backscatter exhibits an aspect ratio of ~1:25.

Fig. 8 presents the backscatter cross sections observed for the cirrostratus, pre-warm frontal cloud system observed on Jan. 29-30, 1988. The maximum backscatter cross section of $4.3 \cdot 10^{-5}$ m^{-1} sr^{-1} was observed near 1:30 GMT. Twenty minute averaged optical thickness varied between between .081 and 2.27, while the backscatter phase function varied from .031 - .057 sr^{-1} .

Note the pattern of repeated, overlapping tilted cells evident in the first half of this data set. Optically thick cirrus frequently exhibit similar morphology. Using the mean cloud level wind to translate the temporal coordinate into the spatial domain suggests the cells are inclined at ~7° from the horizontal. A cloud of this type may appear homogeneous to a nadir viewing satellite sensor, but would not exhibit an optical thickness dependent only on the secant of the view angle. Wind-drift estimates indicate the cells were ~30-50 km wide producing height to width aspect ratios of ~ 1:10. Patterned departures from inverse-cosine-law behavior can have implications for radiative heat balance calculations and for the calibration of wide beam radiometers.

e. *Particle microphysics*

Cirrus sometimes form plate-like crystals which fall flat-face-down because of aerodynamics. In scanning through the zenith, the VIL has observed specular backscatter enhancements by a factor of at least 13, and larger enhancements seem possible. The e^{-1} full width of the forward scatter diffraction peak in one of these observations was ~1.5° (at 1.06 μm) suggesting a minimum crystal diameter of ~50 μm. Some VIL cross sections have revealed thin (<200 m) layers exhibiting specular reflection immediately adjacent to similar layers which do not show specular backscatter enhancements. This suggests the microphysical properties of cirrus are quite heterogeneous. Because of the three dimensional heterogeneity of cirrus, the scientific yield from future experiments could be enhanced by a real time mapping of extended volumes around insitu microphysical measurements. Such mapping might even be used as an element in the selection and execution of flight plans.

Because of this potential for specular backscatter, the HSRL has been operated 3° - 5° from zenith, minimizing the impact of this effect on the measurements of backscatter phase function and backscatter cross section.

NOTE: Summary, References and Figures 3 - 8 may be found in:
part II of Grund and Eloranta ... see poster presentation section.

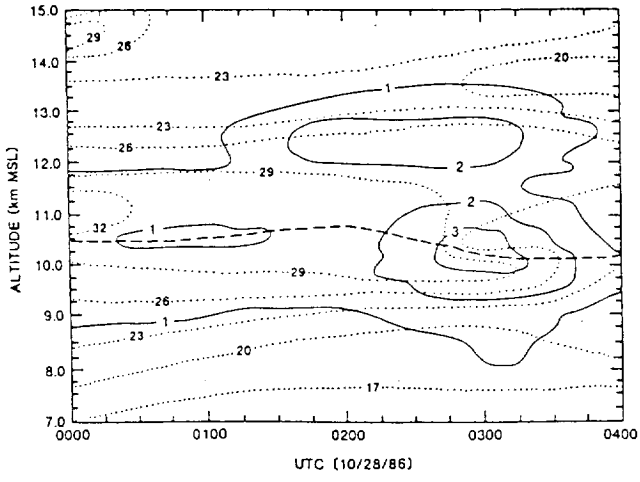

Fig. 1 Background veils of enhanced backscatter have been observed at cirrus altitudes even when cirrus are not present. This layer had an average optical thickness of ~.01. Backscatter cross section (——) in 10^{-7} m^{-1} sr^{-1}, optical mid-cloud altitude (- - -), wind speed (· · ·) in m/s. Note pattern correlations between wind speeds and backscatter cross section.

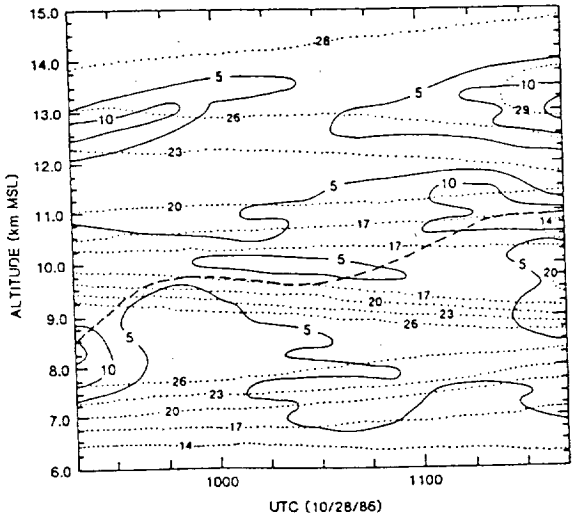

Fig. 2 A 2-layer region of enhanced backscatter. Average optical thickness was ~.003. Backscatter cross section (——) in 10^{-8} m^{-1} sr^{-1}, optical mid-cloud altitude (- - -), wind speed (· · ·) in m/s. Although wind profiles differ from fig. 1, correlations between wind and backscatter are still evident.